Numerical Modelling of Tidal Sediment Dynamics in the Bay of Brest over the Holocene: How the Use of a Process-Based Model over Paleoenvironmental Reconstitutions can Help Understand Long-term Tidal Deposits?

Matthieu Guillaume Olivier[a,b,c*], Estelle Leroux[d], Didier Granjeon[c], Pierre Le Hir[b], Marina Rabineau[d], Pascal Le Roy[a], Laure Simplet[e], Axel Ehrhold[a], Héloïse Muller[b]

a IFREMER/IUEM – ASTRE laboratory – UMR Geo-Ocean – Pointe du Diable, 29280 Plouzané, France

b IFREMER – DYNECO/DHYSED laboratory – Pointe du Diable, 29280, Plouzané, France

c IFP Énergies nouvelles – 1 et 4, avenue de Bois-Préau, 92500, Rueil-Malmaison, France

d IFREMER/IUEM – GIPS laboratory – UMR Geo-Ocean – Pointe du Diable, 29280 Plouzané, France

e IFREMER/IUEM – ODYSC laboratory – UMR Geo-Ocean – Pointe du Diable, 29280 Plouzané, France

Supplementary materials

Supplementary materials of this article contain 13 figures. Figure 1 aims to give an over view of bottom current velocities evolution over the scenarios and displays the impact of rivers water discharges modifications. Figure 2 also displays the impact of rivers modifications, but on bathymetric evolution of scenario 1. Figure 3 shows the evolution of suspended sediment volume over spring tides and highlights the tidal asymmetry in the Bay of Brest. Figures 4 to 9 are the core logs (corelated with seismic profiles) used for the validation of grain size classes distribution. Finally, Figures 10 to 13, and the text included with those figures, detail the comparison between grain size classes erosion and deposition simulated and sediment records.

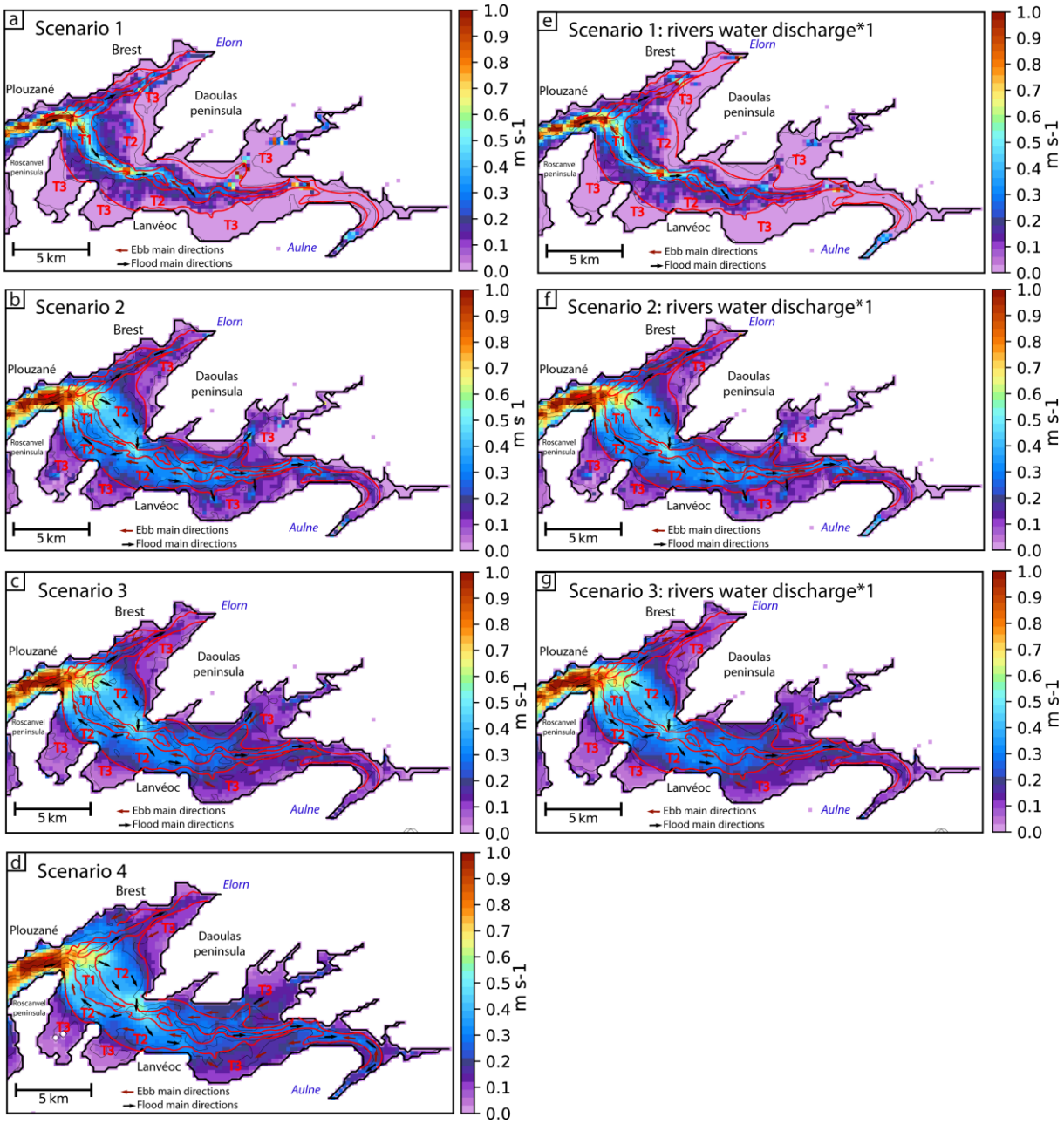

Fig. 1: Bottom current percentile 90 over one year for a: scenario 1, b: scenario 2, c: scenario 3, d: scenario 4, e: scenario 1 with a water river discharge equal to scenario 4, f: scenario 2 with a water river discharge equal to scenario 4, g: scenario 3 with a water river discharge equal to scenario 4.

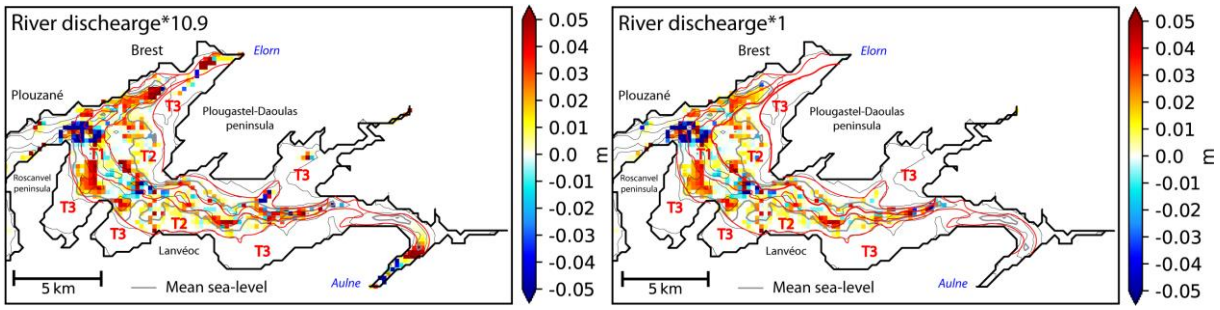

Fig. 2: On the left, bathymetric evolution after 1 year for scenario 1 (9 ka BP) and on the right bathymetric evolution after 1 year for scenario 1, with a river water discharge equal to scenario 4. Red lines are morphological domain limits (T1, T2 T3) and the black line is the present-day coastline. Grey lines represent the mean sea level (-26 m).

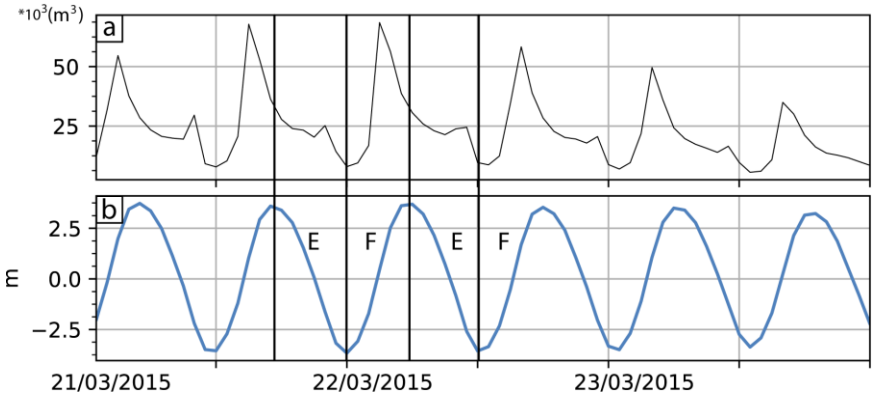

Fig. 3: (a) Evolution of suspended matter volume over the Bay through time over spring tides for the present-day configuration (scenario 4, computational limits on Fig. 3 of the manuscript). (b) Evolution of sea surface variations at the entrance of the Bay (central area). F: Flood tide; E: Ebb tide.

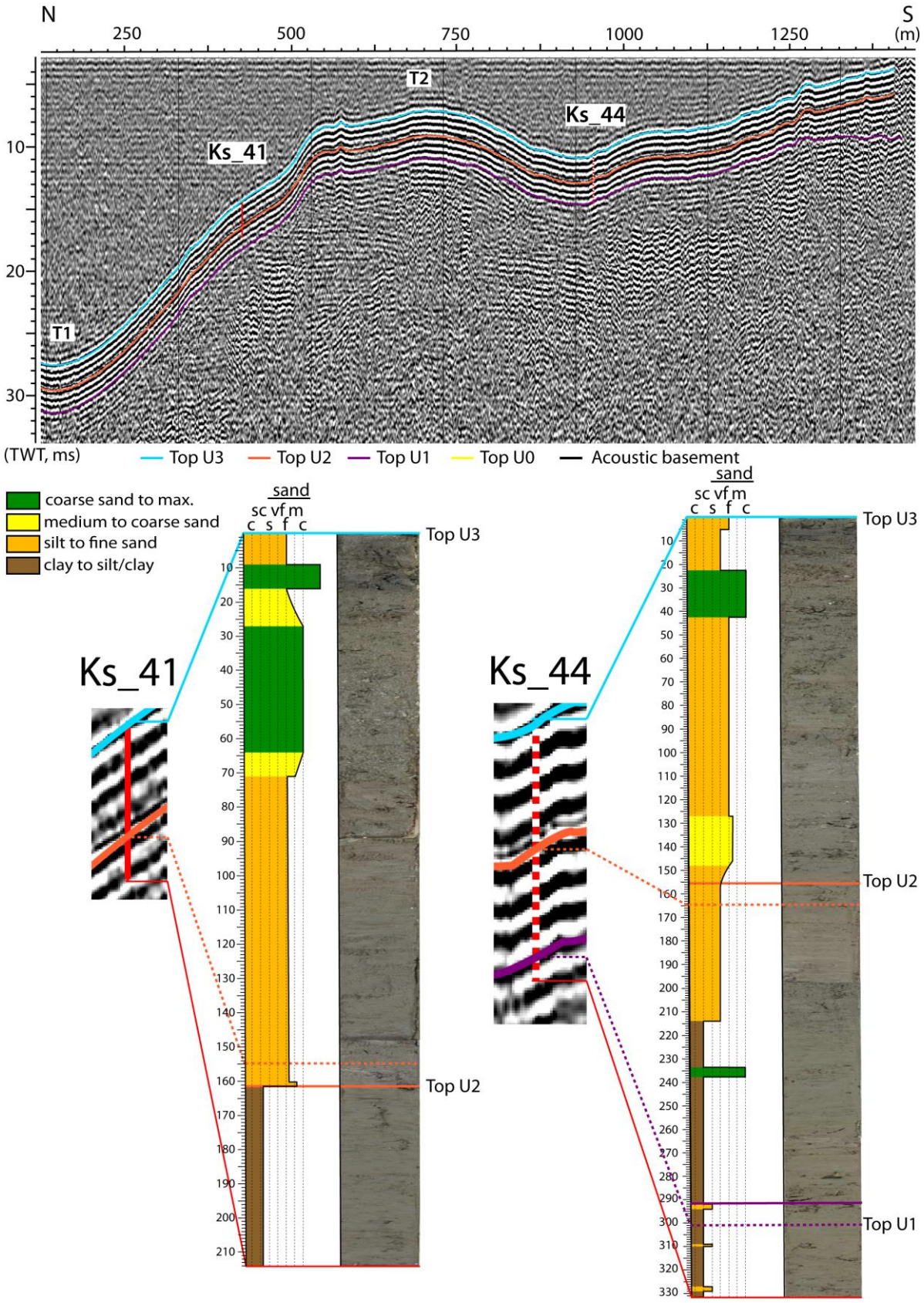

Fig. 4: (top) Interpreted seismic profile (location on Fig. 3b of the manuscript). (bottom) Photographs and lithologic logs for cores Ks_41 and Ks_44. Dashed purple and orange lines are markers from seismic interpretation and full purple and orange lines represent the interpreted top of U1 and U2 (made to compensate the difference of resolution between cores and seismic profile).

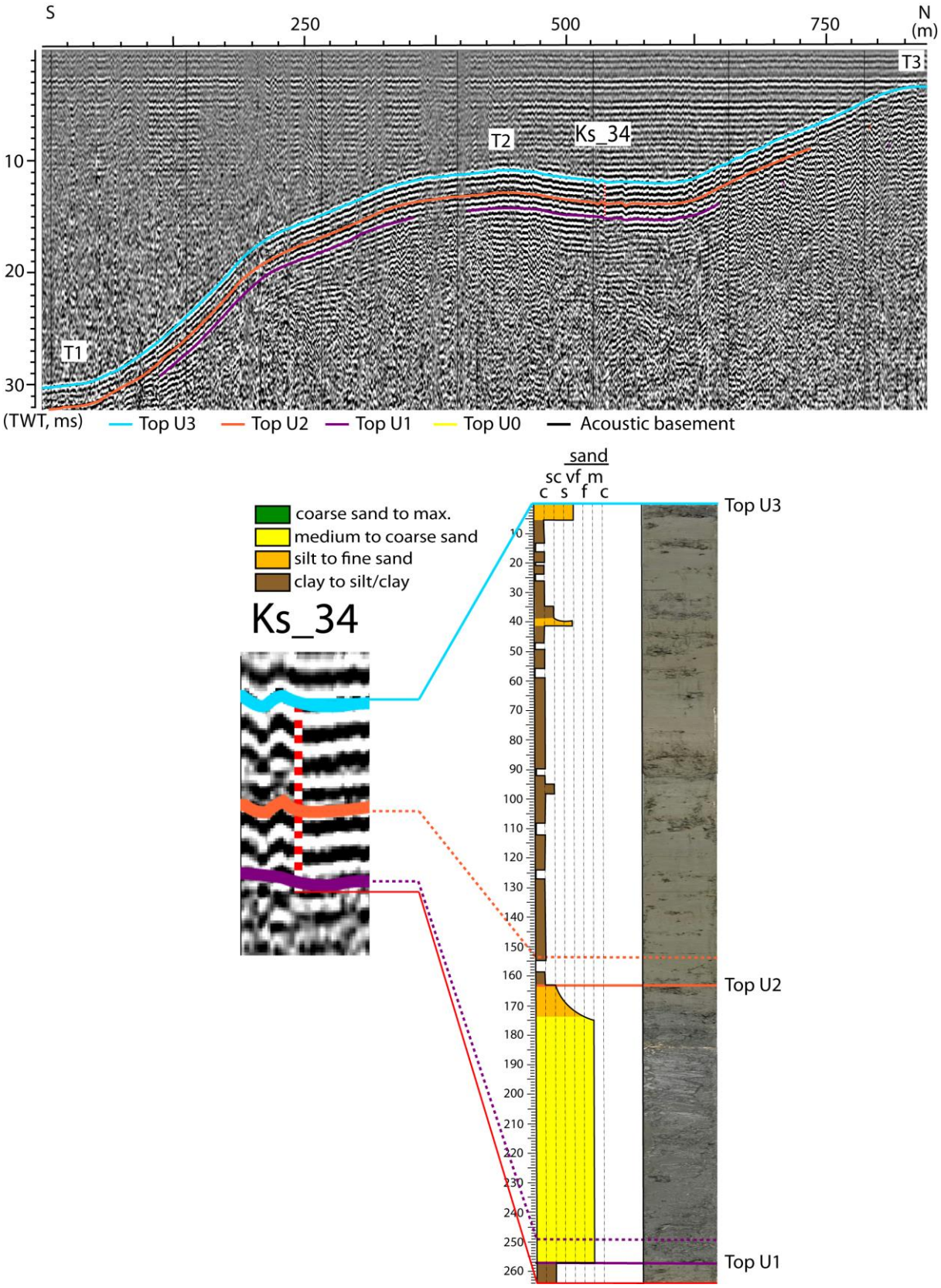

Fig. 5: (top) Interpreted seismic profile (location on Fig. 3b of the manuscript). (bottom) Photograph and lithologic logs for cores Ks_41 and Ks_44. Dashed purple and orange lines are markers from seismic interpretation and full purple and orange lines represent the interpreted top of U1 and U2 (made to compensate the difference of resolution between cores and seismic profile).

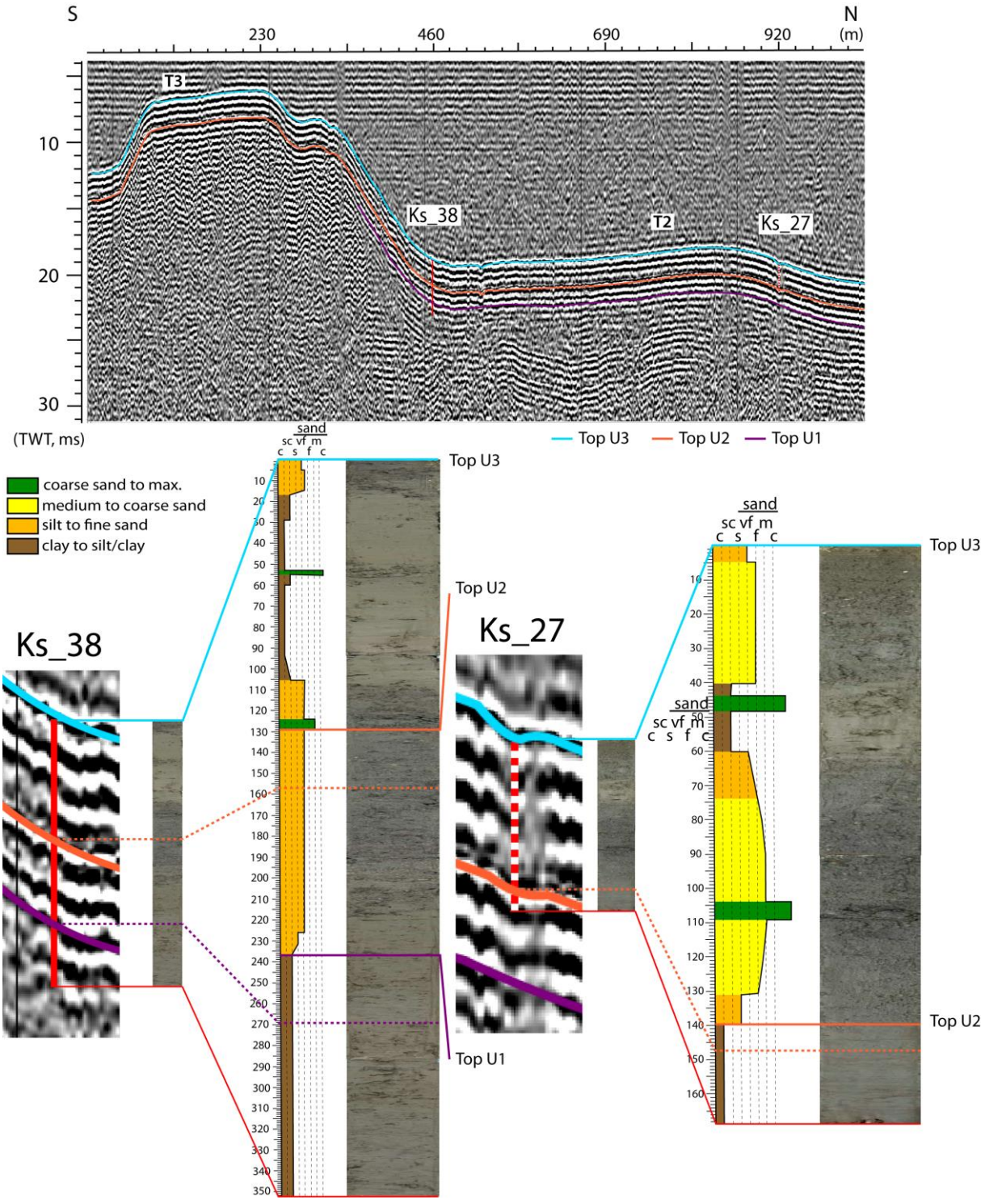

Fig. 6: (top) Interpreted seismic profile (location on Fig. 3b of the manuscript). (bottom) Photographs and lithologic log for cores Ks_38 and Ks_27. Dashed purple and orange lines are markers from seismic interpretation and full purple and orange lines represent the interpreted top of U1 and U2 (made to compensate the difference of resolution between cores and seismic profile).

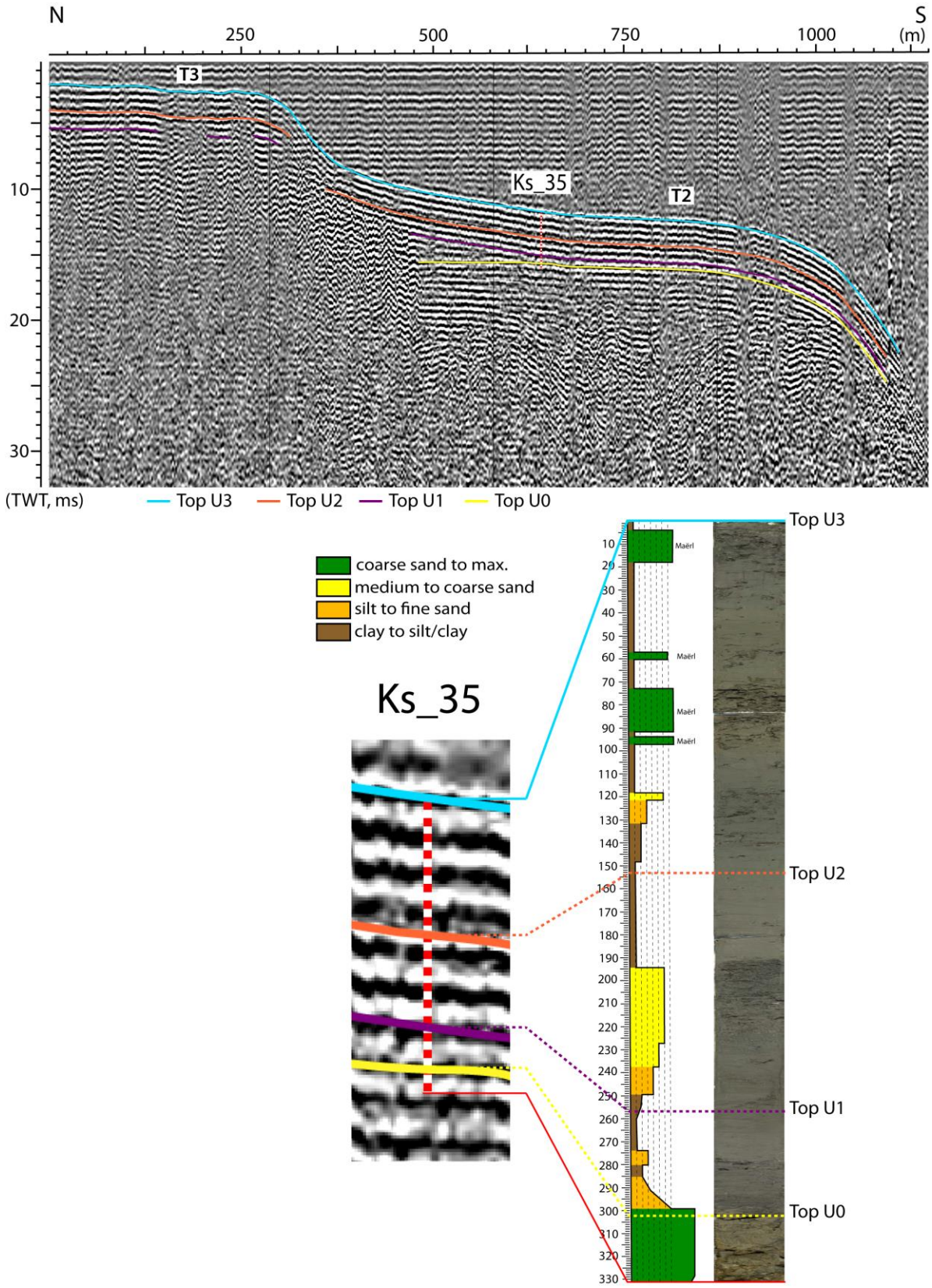

Fig. 7: (top) Interpreted seismic profile (location on Fig. 3b of the manuscript). (bottom) Photograph and lithologic log for core Ks_35. Maërl: only bioconstructions of Maërls.

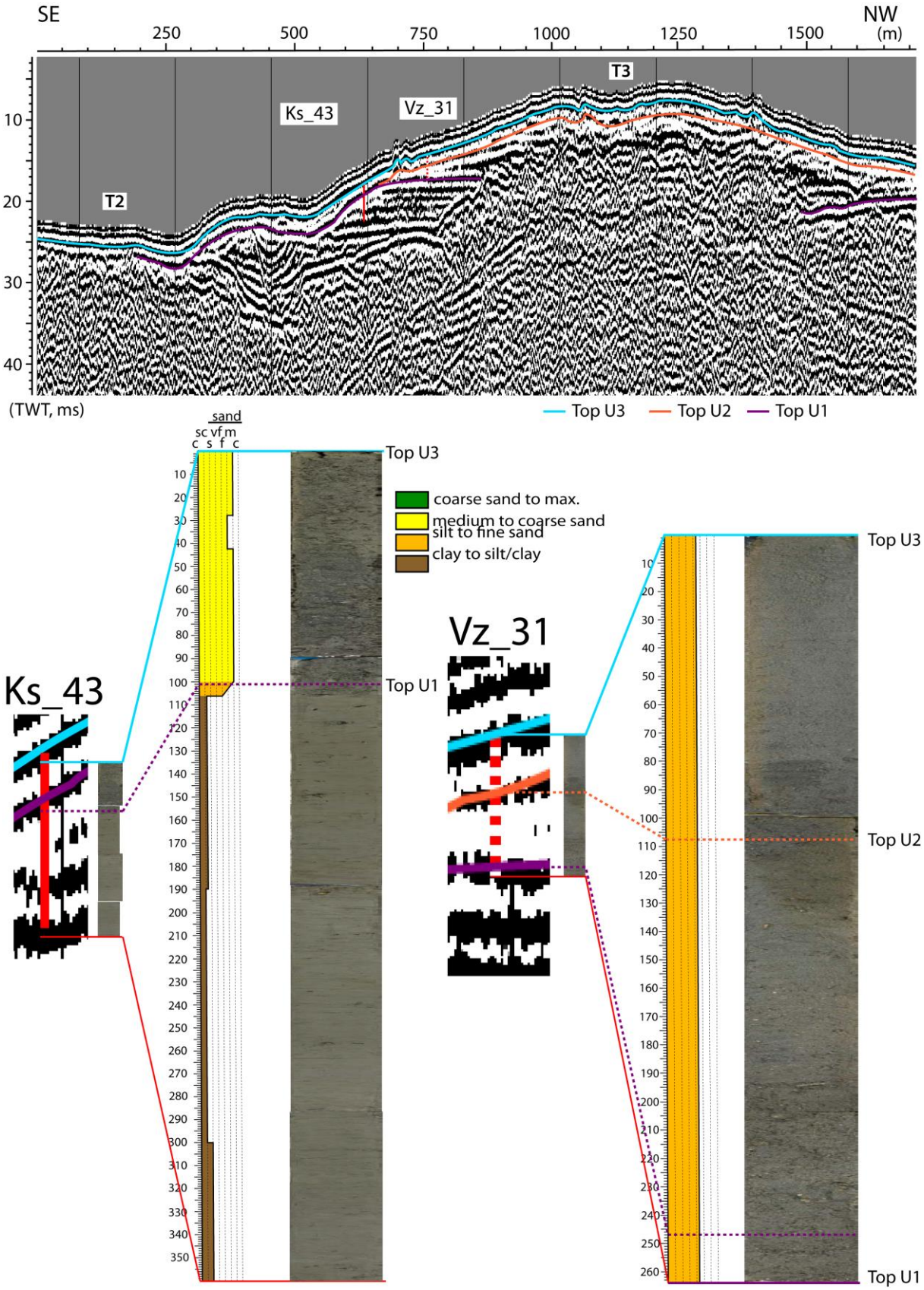

Fig. 8: (top) Interpreted seismic profile (location on Fig. 3b of the manuscript). (bottom) Photographs and lithologic log for cores Ks_43 and Vz_31.

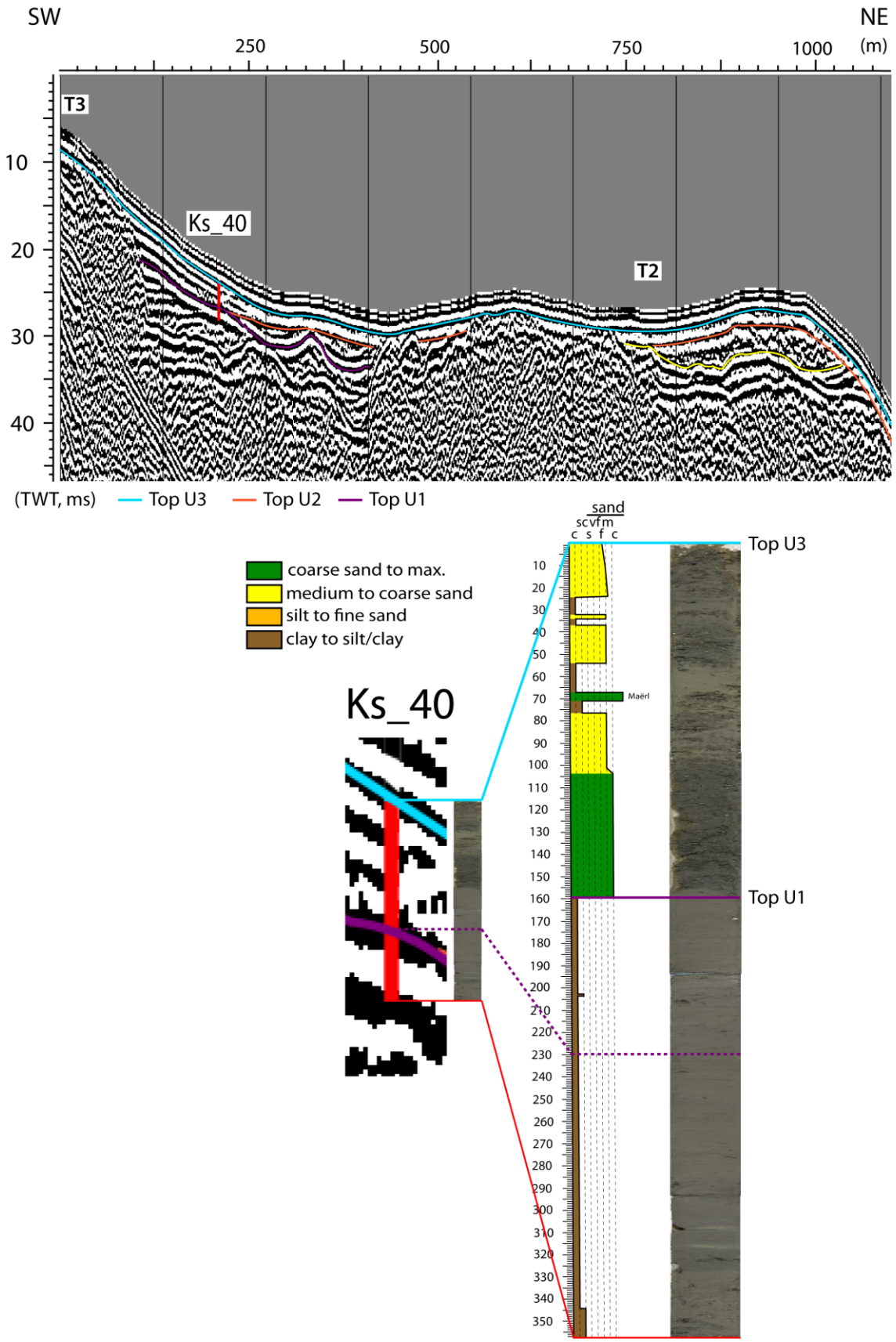

Fig. 9: (top) Interpreted seismic profile (location on Fig. 3b of the manuscript). (bottom) Photograph and lithologic log for core Ks_40. Dashed purple line is marker from seismic interpretation and full purple line represents the interpreted top of U1 (made to compensate the difference of resolution between cores and seismic profile). Maërl: only bioconstructions of Maërls.

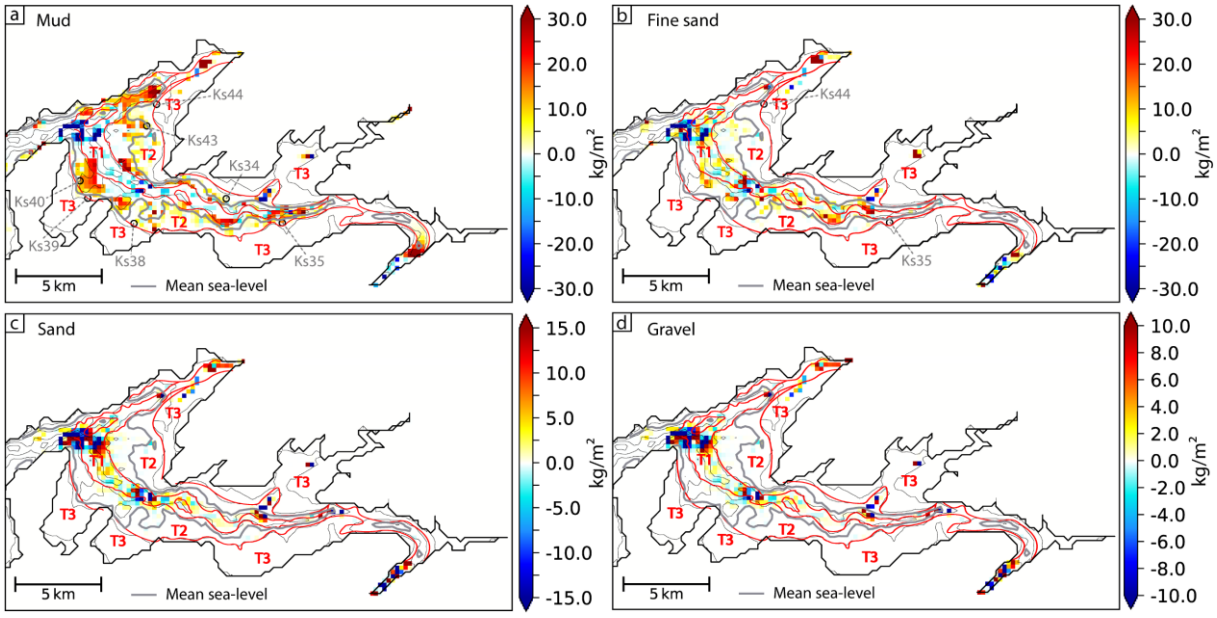

Fig. 10: Grain-size class erosion and deposition after 1 year for scenario 1 (9 – 7.5 ka BP): a mud, b fine sand, c sand, d gravel. Black circles show where the corresponding grain-size classes were recorded by cores. Core names are available in grey and red lines are morphological domain limits.

At each core location or very close (one cell of the computation grid) where muds are observed, mud deposits are simulated (Fig. 10a, Tab. 6 of the manuscript, Ks_34, Ks_35, Ks_38, Ks_39, Ks_40, Ks_43 and Ks_44). All non-cohesive sediment classes (fine sand, sand and gravel) are mostly present over T1, only some fine sands are present in secondary channels and reach some areas of T2 (Figs. 10b, 10c, 10d). Unfortunately, cores are available mostly at the interface between T2 and T3. However, two cores present fine sand accumulations (Ks_35 and Ks_44) and no fine sand deposit is simulated at the beginning of U1 at these locations (Fig. 10b).

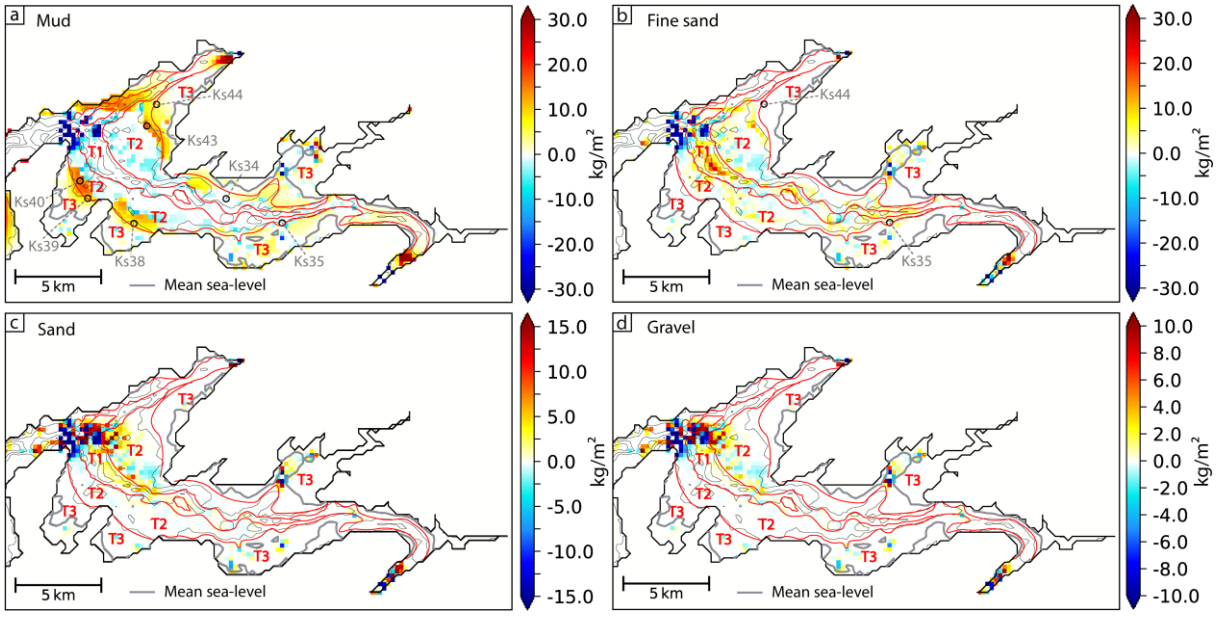

Fig. 11: Grain-size class erosion and deposition after 1 year for scenario 2 (7.5 – 7 ka BP): a mud, b fine sand, c sand, d gravel. Black circles show where the corresponding grain-size classes were recorded by cores. Core names are available in grey and red lines are morphological domain limits.

All the cores presenting mud records (Fig. 11a, Ks_38, Ks_39, Ks_40, Ks_43 and Ks_44) are located where mud deposits are simulated, except for Ks_34 and Ks_35. At Ks_34 and Ks_35 locations, the balance between erosion and deposition is close to 0 (Fig. 11a), but mud deposits are simulated during scenario 1 (Fig. 10a). If no erosion is simulated during scenario 2 (end of U1), deposits from the beginning of U1 (scenario 1) should be preserved and are indeed observed inside cores (Ks_34 and Ks_35). Cores on slopes between T2 and T3, do corroborate this simulation result as they display only mud and fine sand. Fine sand deposit is observed in Ks_44 and is simulated close to the ks_44 location. In the upper area, slight movements of sand and gravel are simulated over T1 and secondary channels, but over these areas, only fine sands are deposited over T1 and secondary channels in smaller quantity than in the centre (around 5 kg/m², Figs. 11b, 11c, 11d). Fine sands are observed inside core Ks35, which is located in a secondary channel in the upper area (Fig. 11b). Deposits simulated in T1 are impossible to confirm by field data as no cores are available in this morphological domain. However, the seismic facies were interpreted as coarse sediments (Gregoire, 2016) and would therefore corroborate the simulation results.

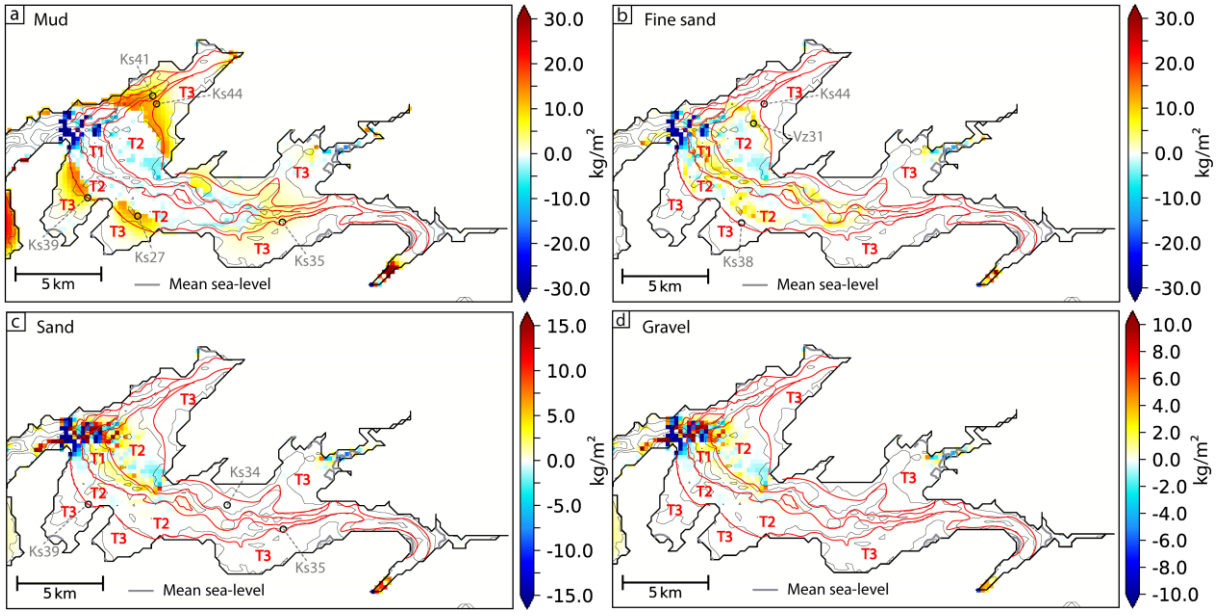

Fig. 12: Grain-size class erosion and deposition after 1 year for scenario 3 (6.8 – 3 ka BP): a mud, b fine sand, c sand, d gravel. Black circles show where the corresponding grain-size classes were recorded by cores. Core names are available in grey and red lines are morphological domain limits.

Mud deposits are recorded in Ks_35, but the two cores available in the upper part also display sands (Ks_34 and Ks_35, Fig. 12c). Mud deposits are also observed in cores Ks_27, Ks_39, Ks_41 and Ks_44 in the centre (Fig. 12a), where mud deposits are simulated. Observations of cores Ks_38, Ks_39, Ks_44 and Vz_31 show fine sands and sand on slopes between T2 and T3 and fine-sand deposits are simulated close to the three core locations (Fig. 12b). Ks_39 reveals the presence of some sand on the slope between T2 and T3, but very few deposits of sand are simulated close to core Ks_39 (Fig. 12c, less than 1 kg/m²).

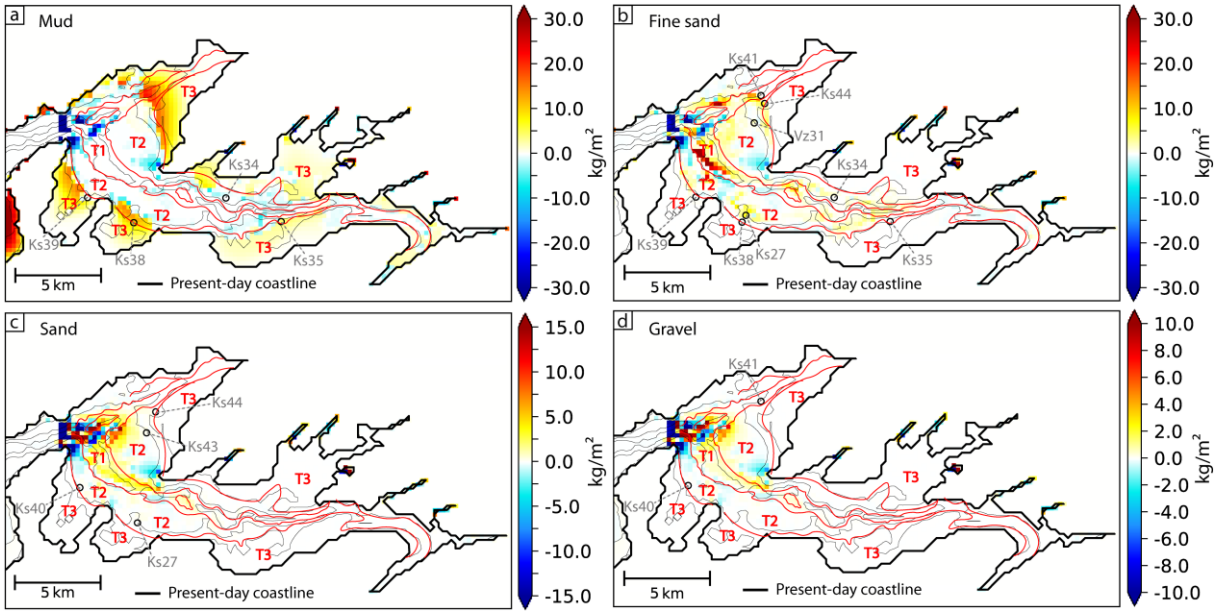

Fig. 13*: Grain-size class* erosion and deposition *after 1 year for scenario 4 (present-day): a mud, b fine sand, c sand, d gravel. Black circles show where the corresponding grain-size classes were recorded by cores. Core names are available in grey and red lines are morphological domain limits.*

Muds are observed only in Ks_35, Ks_38, Ks_39 (T3) and Ks_34 (T2), but at the Ks_34 location, no mud deposit is simulated. Fine-sand deposits are simulated close to cores that also show fine-sand (Fig. 13b, Ks_27, Ks_34, Ks_35, Ks_38, Ks_39, Ks_41, Ks_44, Vz_31). Sands simulated and observed in cores (Ks_27, Ks_40, Ks_43, Ks_44) also make a good match, even if small quantities are simulated at these core locations (around 1 kg/m², Fig. 13c). Also note that two cores (Ks_40 and Ks_41) show gravel deposit that is not simulated, close to T1 in the north of the central part and on slopes between T2 and T3 in the south. The presence of gravel deposits in two cores is unexplained by the tidal process.

Global trends of erosion/deposition patterns between simulation and data fit well. However, there are some mismatches between the simulations and the geological data: the presence of sands (observed in Ks_34 and Ks_35) in the upper zone during scenario 3 and gravels (observed in Ks_40 and Ks_41) in the centre during scenario 4 remains unexplained by simulations (Figs. 12 and 13 respectively). Simulated tidal currents are not able to transport sands and gravels at these core locations, and therefore it is difficult to link such coarse deposits to tide-induced hydrodynamics (Olivier et al., 2021, Figs. 12 and 13). They are potentially due to non-simulated extreme events, such as storm winds. Such energetic events could be able to transport coarse sediments into the Bay, without later remobilisation by weaker tide-induced currents. They should therefore be recorded in the cores (unless they reach T2 in the centre, which is the only morphological domain where tidal currents can transport sands and gravels during scenarios 2, 3 and 4). Ehrhold et al. (2021) observed storm patterns within some sedimentary facies of units U2 and U3 that may correspond to the coarsest deposits we also observed. The presence of these coarse sediments underlines the importance of climatic variations on sediment supply in estuaries.

References

Ehrhold, A., Jouet, G., Le Roy, P., Jorry, S.J., Grall, J., Reixach, T., Lambert, C., Gregoire, G., Goslin, J., Roubi, A., Penaud, A., Vidal, M., Siano, R., 2021. Fossil maerl beds as coastal indicators of late Holocene palaeo-environmental evolution in the Bay of Brest (Western France).

Gregoire, G., 2016. Dynamique sédimentaire et évolution holocène d'un système macrotidal semi-fermé. l'exemple de la rade de Brest, Brest, p. 294.